TRAFFIC JAM DYNAMICS IN A CAR-FOLLOWING MODEL WITH REACTION-TIME DELAY AND STOCHASTICITY OF DRIVERS

Gábor Orosz [*], **Bernd Krauskopf** [**], **R Eddie Wilson** [**]

[*] *Mathematics Research Institute, University of Exeter, Laver Building, North Park Road, Exeter, EX4 4QE, UK*

[**] *Department of Engineering Mathematics, University of Bristol, Queen's Building, University Walk, Bristol, BS8 1TR, UK*

Abstract: We consider an optimal-velocity car-following model with reaction-time delay of drivers, where the characteristics of the drivers change according to a suitably calibrated random walk. In the absence of this stochasticity we find stable and almost stable oscillations that correspond to stop-and-go traffic jams that eventually merge or disperse. We study how the distribution of the merging times depends on the parameters of the random walk. Our numerical simulations suggest that the motion of the fronts into and out of traffic jams may be subject to a 'macroscopic' random walk.

Keywords: optimal velocity model, reaction-time delay, stop-and-go waves, random walk

1. INTRODUCTION

Stop-and-go traffic jams can often be observed in real-life traffic situations (Kerner, 1999). In such traffic jams high density and low velocities are found, while outside the traffic jams there are free-flow conditions, that is, low density and high (close to the speed limit) velocities. This traffic scenario can be reproduced by so-called car-following models where vehicles are modelled as discrete entities that move in continuous one-dimensional space and time. In such models the reaction-time delay of drivers can be included explicitly (Helbing, 2001). In (Orosz *et al.*, 2004; Orosz *et al.*, 2005) we investigated the stop-and-go solutions in a simple optimal velocity car-following model with drivers' reaction time. The question arises as to whether the dynamics of stop-and-go traffic jams explored in car-following models is robust. Should the inconsistent psychological behaviour of drivers and external disturbances such as weather and road unevenness be taken into account? One approach is to model such influences by stochastic effects. As an initial investigation, in this paper we model drivers' sensitivity parameter with a random walk and study the effect of stochasticity on traffic jam dynamics.

2. MODEL DETAILS

We place n cars on a unidirectional single-lane circular road of length L and consider drivers with identical parameters. (For the sake of simplicity, we mainly restrict ourselves to the representative case of $n = 9$ vehicles in this paper.) The velocity of the i-th vehicle is denoted by v_i and its distance to the preceding $(i+1)$-st vehicle, known as the *headway*, is denoted by h_i. We assume that the acceleration of vehicles is given by

$$\dot{v}_i(t) = \alpha_i(t)\big(\mathrm{V}\left(h_i(t-1)\right) - v_i(t)\big)\,, \quad i = 1, \ldots, n\,, \tag{1}$$

where dot refers to the derivative with respect to the time t; that is, each driver approaches an *optimal velocity* (OV), given by the function $\mathrm{V}(h) \geq 0$ so that they react to their headway

via a *reaction-time delay* which here is rescaled to one. The sensitivity α_i of each vehicle fluctuates around the *average sensitivity* α. The quantity $1/\alpha$ gives the characteristic relaxation time for approaching the optimal velocity $\mathrm{V}(h)$.

Further, we consider the ring-road kinematic conditions

$$\begin{aligned} \dot{h}_i(t) &= v_{i+1}(t) - v_i(t)\,, \quad i = 1, \ldots, n-1\,, \\ \dot{h}_n(t) &= v_1(t) - v_n(t)\,. \end{aligned} \tag{2}$$

Note that the length of the ring enters via the constraint $\sum_{i=1}^{n} h_i = L$.

In this paper we use the continuously differentiable, nonnegative, and monotone increasing *OV function*

$$\mathrm{V}(h) = \begin{cases} 0\,, & \text{if} \quad 0 \le h \le 1\,, \\ v^0 \dfrac{(h-1)^3}{1+(h-1)^3}\,, & \text{if} \quad h > 1\,, \end{cases} \tag{3}$$

which has a sigmoidal shape. Note that $\mathrm{V}(h) \to v^0$ as $h \to \infty$, where v^0 is known as the *desired speed*, which corresponds to the (high) free-flow speed of drivers when traffic is sparse. Furthermore, $\mathrm{V}(h) \equiv 0$ for $h \in [0, 1]$, so that 1 is the rescaled *jam headway*. If a vehicle's headway becomes less than 1 it will attempt to come to a stop.

The above model with constant sensitivity $\alpha_i(t) \equiv \alpha$ for $i = 1, \ldots, n$ was investigated by analytical and numerical methods in (Orosz *et al.*, 2005; Orosz and Stépán, 2006). In this paper we assume that drivers change their behavior stochastically which we model by assuming that each sensitivity α_i is subject to a biased random walk around the average sensitivity α:

$$\dot{\alpha}_i(t) = \gamma\big(\alpha - \alpha_i(t)\big) + \kappa\zeta_i(t)\,, \quad i = 1, \ldots, n\,. \tag{4}$$

Here ζ_i is assumed to be white (uncorrelated) Gaussian noise, that is,

$$\overline{\zeta_i(t)} = 0\,, \quad \overline{\zeta_j(t)\zeta_k(s)} = \delta_{jk}\,\delta(t-s)\,. \tag{5}$$

The overbar stands for averaging, $1/\gamma$ is a *relaxation time* for the random walk, and κ is the *noise strength*.

Equations (1), (4), and (2) constitute a system of stochastic delay differential equations (SDDEs). For the special case of $\kappa = 0$, $\gamma \to \infty$ equation (4) simplifies to $\alpha_i(t) \equiv \alpha$ for $i = 1, \ldots, n$. Thus, stochasticity is eliminated and equations (1) and (2) constitute the system of delay differential equations (DDEs) studied in (Orosz *et al.*, 2005; Orosz and Stépán, 2006). First, we investigate the dynamics of traffic jams in this deterministic system in Section 3. Then, in Section 4, we study how the dynamics changes when the parameters γ and κ are tuned. Finally, we conclude and discuss some future directions of research in Section 5.

3. DETERMINISTIC CASE

For $\alpha_i(t) \equiv \alpha$ for $i = 1, \ldots, n$ equations (1) and (2) are deterministic and can be studied with tools from analytical and numerical bifurcation theory. We summarize some of the results shown in (Orosz *et al.*, 2005; Orosz and Stépán, 2006) which are necessary for understanding the further investigation of the system.

It is possible to investigate analytically the linear stability of the *uniform flow equilibrium*

$$h_i(t) \equiv h^* = L/n\,, \quad v_i(t) \equiv \mathrm{V}(h^*)\,, \quad i = 1, \ldots, n\,, \tag{6}$$

where the parameter h^* is called the *average headway*. Varying this parameter one may find Hopf bifurcation points where small amplitude oscillations can appear, which correspond to travelling waves with discrete wave numbers $k = 1, \ldots, n/2$ (even n) or $k = 1, \ldots, (n-1)/2$ (odd n). Further, it is possible to determine the branches of oscillations originating in these Hopf points when the parameter h^* is varied. Close to the Hopf points the oscillations can be obtained analytically by using normal form calculation, while far from the Hopf points they can be followed with numerical continuation. Note that both stable and unstable oscillations can be found in this way. There are parameter ranges where the oscillations belonging to different wave numbers may coexist with each other and with the uniform flow equilibrium. For such parameters, the $t \to \infty$ behavior may depend on the initial condition.

In Fig. 1 oscillations for wave numbers $k = 1, 2$ are shown for parameter values where the uniform flow equilibrium is unstable; they were found with the continuation package DDE-BIFTOOL (Engelborghs *et al.*, 2001). On the left the time profiles of velocity and headway oscillations are displayed while on the right they are shown in the headway velocity phase plane. Only the oscillations for the first car are displayed since the oscillations for the other vehicles are copies that are shifted by $\frac{k}{n}T_\mathrm{p}$ where T_p is the period. Hence, travelling wave solutions are obtained that propagate against the flow of vehicles.

When the wave number k is relatively small compared to the car number n ($k = 1, 2$ is small in this case) stop-and-go oscillations appear. That is, there are high and low (practically zero) velocity plateaux that are connected by stop-fronts (connecting a high velocity to an almost zero velocity) and *go-fronts* (connecting an almost zero velocity to a high velocity). Indeed, the headway oscillations possess similar features. Such periodic orbits have a shape similar to a heteroclinic orbit in the phase plane. However, the period T_p is finite and approximately proportional to $1/k$, as is demonstrated by the red dashed vertical lines. As the wave number is increased the time spent in the plateaux becomes smaller while the stop-fronts and the go-fronts remain similar.

It is possible to investigate the stability of these oscillations with DDE-BIFTOOL via the Floquet multipliers of the periodic solutions. Floquet multipliers measure the expansion or contraction of a vector over one period as the flow is followed along the periodic orbit. A periodic solution is

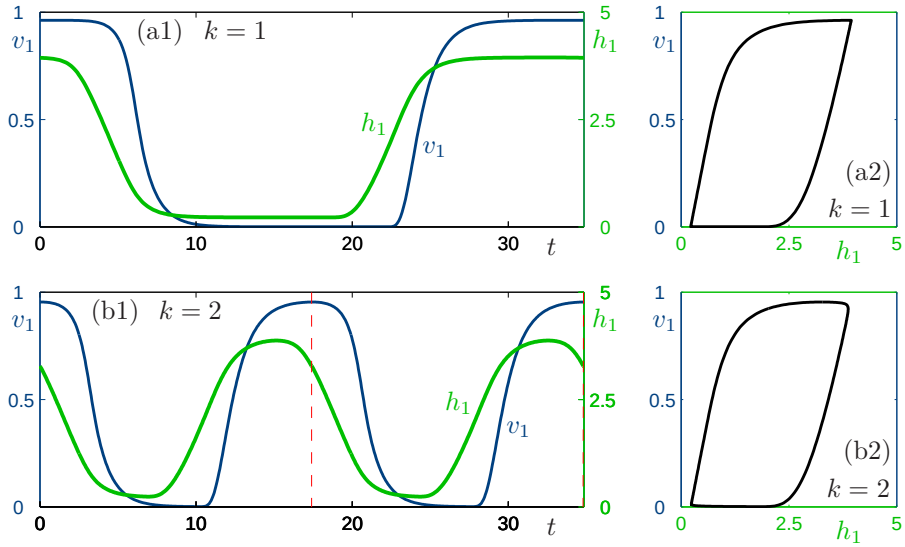

Fig. 1. Oscillations for $n = 9$ cars for wave numbers $k = 1, 2$. On the left-hand side, the velocity v_1 of the first car is shown in dark blue to the scale on the left; the headway h_1 of the first car is shown in green to the scale on the right; the oscillations are shown on the scale of one period of $T_\mathrm{p} \simeq 34.84$ for $k = 1$ and the period of $T_\mathrm{p} \simeq 17.41$ for $k = 2$ is indicated by the red dashed vertical lines. On the right-hand side, the oscillations are shown in (h_1, v_1) plane. The desired speed is $v^0 = 1.0$, the sensitivity is $\alpha = 1.0$, and the average headway is $h^* = 2.0$.

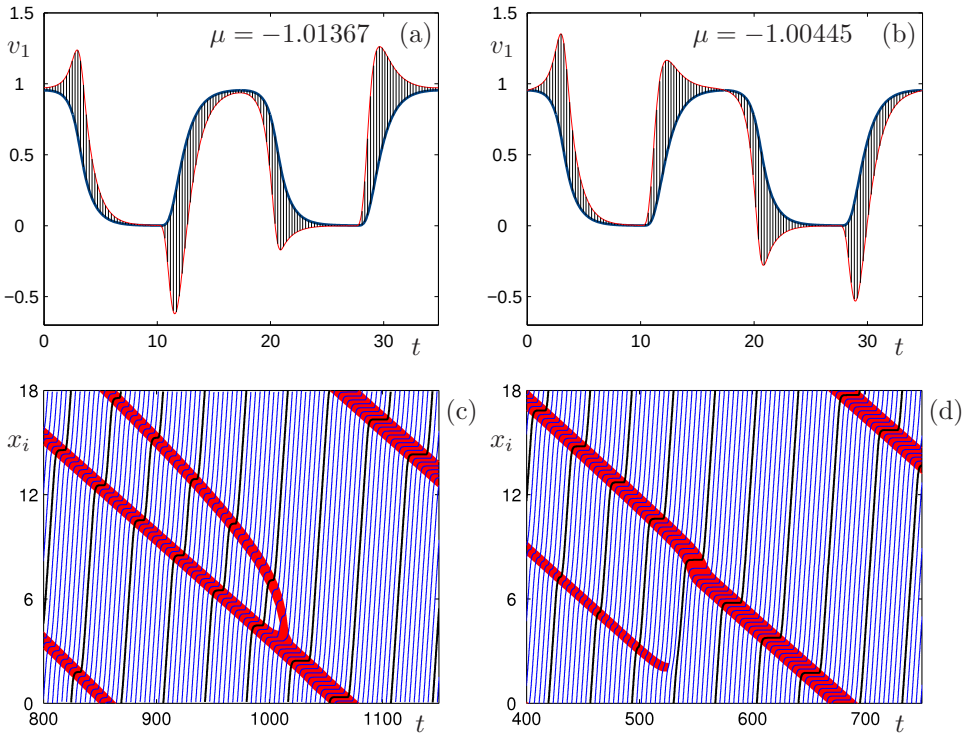

Fig. 2. Panels (a) and (b) show the eigendirections in the form of a direction fields plotted over twice the period of the periodic solution as projections onto the velocity v_1 of the first car for the periodic solution $k = 2$ and $n = 9$. The red curves show the corresponding modulated solutions. Panels (c) and (d) display the positions x_i of all $n = 9$ cars when two traffic jams merge and when a traffic jam disperses, respectively. The trajectory of the first car is emphasized in black and traffic jams are indicated in red when the velocity drops below $v^0/3$. Panel (a) corresponds to the merging of traffic jams as shown in panel (c), while panel (b) corresponds to dispersion of one of the traffic jams as depicted in panel (d). The parameters are $v^0 = 1.0$, $\alpha = 1.0$, and $h^* = 2.0$.

stable if all Floquet multipliers are inside the unit circle of the complex plane, and unstable if there exists a multiplier outside the unit circle. It turns out that the oscillations and the corresponding travelling wave solutions are only stable for $k = 1$. In other words, for $t \to \infty$ only one wave travels along the circular road, for generic choices of initial data. For $k > 1$ there exist $2k$ multipliers outside the unit circle. However, when the wave number is relatively small compared to n ($k = 2$ in the present case) the unstable Floquet multipliers may be very close to the unit circle

($\mu = -1.01367$ and $\mu = -1.00445$ in this case). Consequently the stop-and-go oscillations are only weakly unstable in the sense that solutions can stay in their vicinity for a long time. That is, oscillations as in Fig. 1(b1) can survive for many periods.

The eigendirections belonging to the unstable Floquet multipliers can be computed and represented by DDE-BIFTOOL in the form of a direction field that shows how a vector changes along the periodic orbit under the action of the variational equation (Green *et al.*, 2004). In Fig. 2(a) and (b) we show the unstable direction and the corresponding modulated solution with respect to the velocity profile of the first car. It can be seen that the instability of the periodic orbit is not 'spread evenly' along the periodic orbit, but that it is larger near the fronts and smaller near the plateaux. Notice the difference between the two cases in Fig. 2(a) and (b) in terms of the direction of motion of the modulated fronts. In panel (a) the stop-front and the go-front of a low-velocity plateau move in the same direction and the fronts of one and the other low-velocity plateaux move in opposite directions. In panel (b) the stop-front and the go-front of a given low-velocity plateau move in opposite directions either towards each other or apart.

The results of numerical simulation show that the above front dynamics is responsible for merging or dispersing traffic jams. In Fig. 2(c) and (d) the positions of all vehicles are plotted in time. The low-velocity regions (i.e., the traffic jams) can be found where the gradient of the position curves is small; this is highlighted in red. It can be seen that two stop-and-go waves are formed by the collective motion of vehicles, and they persist for a long time before they either merge or one of them disperses. Indeed, stop-fronts and go-fronts can be identified in these figures where vehicles enter and leave the traffic jams. These fronts move with approximately the same speed, that is, they move slowly relative to each other. When the fronts of a given traffic jam move in the same direction and the traffic jams move in opposite directions they merge as shown in Fig. 2(c). When the fronts of a given traffic jam move in opposite directions one of the traffic jams disperses while the other becomes slightly wider. Whether merging or dispersion occurs and when it happens depends on the initial condition. However, one may expect that merging is more dominant since the Floquet multiplier belonging to this behavior is larger. In the next section we investigate the dynamics of fronts changes when stochasticity is introduced into the system.

4. MERGING TIME DISTRIBUTION

We now investigate the system of stochastic delay differential equations (1), (2), (4) considering finite constants $\kappa, \gamma > 0$ in (4) which governs the random walk of the sensitivities α_i. Here we study the case when in the deterministic limit $\kappa = 0$, $\gamma \to \infty$, the two traffic jams merge. Thus, in the remainder of this paper we use the initial conditions used in Fig. 2(c).

Equation (4) is sometimes called an Ornstein-Uhlenbeck process, and the solution for the distribution of α_i can be obtained from the related Fokker-Planck equation; see (Finch, 2004). In particular, the (stable) equilibrium distribution of α_i is given by

$$p^{\mathrm{eq}}(\alpha_i) = \sqrt{\frac{\gamma}{\kappa^2 \pi}}\, \mathrm{e}^{-\frac{\gamma}{\kappa^2}(\alpha_i - \alpha)}, \quad i = 1, \ldots, n\,. \tag{7}$$

By using this as an initial distribution for α_i, stochastic transients are eliminated. Note that drivers are still considered to be identical in the sense that all α_i fluctuate around the same mean value with the same variance according to the same distribution.

We keep the quantity $\kappa^2/\gamma = 0.01$ fixed in order to keep the equilibrium distribution (7) of α_i unchanged. Thus, by increasing the noise strength κ the relaxation time $1/\gamma$ of the random walk decreases. Two realizations of the random walk are shown in Fig. 3(a1) and (b1) for the sensitivity of the first vehicle. Notice that the random variable changes between approximately the same boundaries in both cases, but drivers change their sensitivity less rapidly in panel (a1) since the relaxation time is ten times larger.

The corresponding dynamics of traffic jams are depicted in Fig. 3(a2) and (b2). One can see that the noise effects do not destroy the qualitative dynamics of traffic jams, i.e., two traffic jams appear and persist for a long time before they either merge or one of them disperses. However, the front motions become 'noisy' even thought the trajectories of individual vehicles are still smooth. In both cases the sane initial condition is used as in Fig. 2. In other words, the traffic jams are 'set to merge'. In correspondence to this initial condition, most of the realizations lead to the merging of traffic jams, as shown in Fig. 3(a2), but, due to the stochasticity, some of the realizations result in dispersion of one of the traffic jams, as depicted in Fig. 3(a2). Furthermore, the time T_{m} needed for merging/dispersion differs for each realization; compare the horizontal scales in Fig. 3(a2) and (b2).

In order to obtain a quantitative description of how the merging/dispersion time T_{m} changes we computed its distribution obtained by 5000 realizations. This is shown in the panels of Fig. 4 for different values of parameters κ and γ. It can be seen that the most probable merging/dispersion time $T_{\mathrm{m}}^{\mathrm{MP}}$, given by the position of the maximum of the distribution, is smaller than the deterministic merging time (red vertical line) but the merging time distribution has an exponential-like tail. According to the literature of passage-time distributions (Noskowicz and Goldhirsch, 1990), this distribution suggests that on the top of the macro-

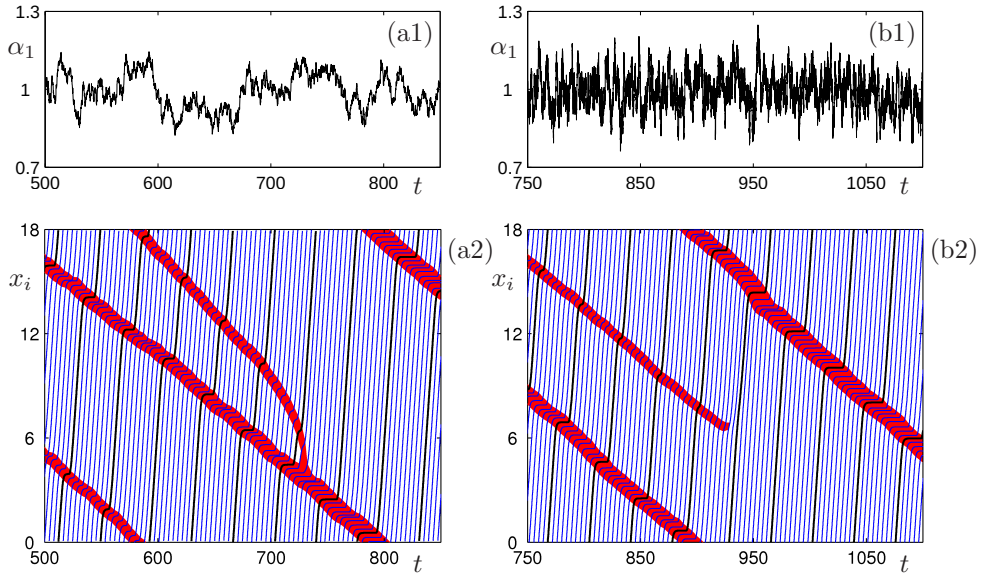

Fig. 3. Random walks of sensitivity α_1 of the first car are shown in panels (a1) and (b1); and the corresponding positions x_i of all $n = 9$ cars in panels (a2) and (b2) so that the trajectory of the first car is emphasized in black and traffic jams are indicated in red when the velocity drops below $v^0/3$. The parameters $\kappa = 0.0316$, $\gamma = 0.1$ are used in the left side and the parameters $\kappa = 0.1$, $\gamma = 1$ in the right side. The other parameters are $v^0 = 1.0$, $\alpha = 1.0$, and $h^* = 2.0$. Both simulations were started with the initial condition corresponding to Fig. 2(c).

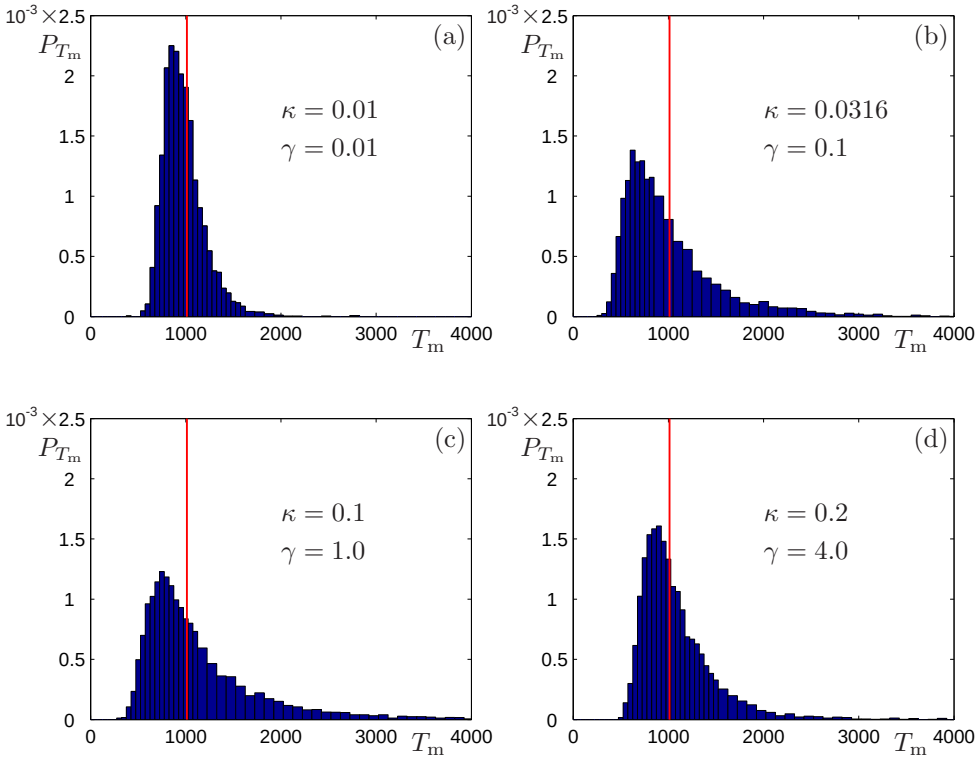

Fig. 4. Distributions of the merging/dispersion time T_m for different values of parameters κ and γ as indicated in each panel. The red vertical lines at $T_\mathrm{m} = 1011.96$ shows the merging time in the deterministic case. The other parameters are $v^0 = 1.0$, $\alpha = 1.0$, and $h^* = 2.0$. All simulations were started from the same initial condition as used in Fig. 2(c).

scopic nonlinear dynamics of the fronts there is a 'macroscopic' random walk, which originated from the 'microscopic' random walk of the sensitivity.

When changing the noise strength κ and the relaxation time γ (so that $\kappa^2/\gamma = 0.01$), both the most probable merging/dispersion time T_m^MP and the standard deviation σ_{T_m} of the merging/dispersion time distribution change as can be seen when comparing the panels of Fig. 4. Increasing κ and γ, the location of the maximum T_m^MP moves first further then closer to the deterministic merging time (red vertical line) and the standard deviation σ_{T_m} first becomes larger than smaller again. This is possible since on the one hand the applied noise is not simple additive noise; and on the other hand

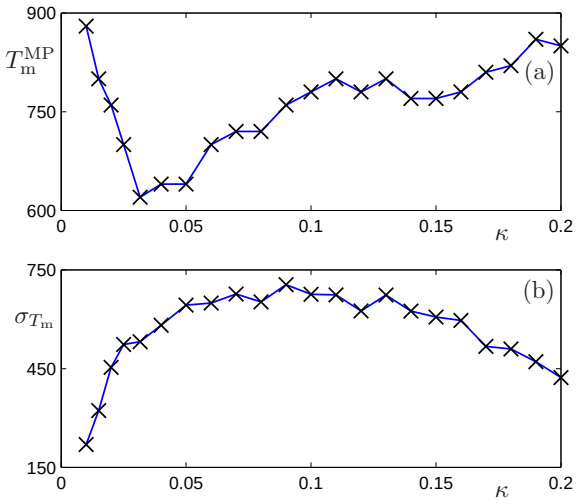

Fig. 5. The most probable merging/dispersion time $T_{\rm m}^{\rm MP}$ (a) and the standard deviation $\sigma_{T_{\rm m}}$ of the merging time distribution (b) as a function of the noise strength κ. The points at $\kappa = 0.01$, $\kappa = 0.0316$, $\kappa = 0.1$, and $\kappa = 0.2$ corresponds to the panels (a)–(d) of Fig. 4. For all values of κ the initial conditions were the same as in Fig. 2.

increasing the noise strength κ and the relaxation time $1/\gamma$ is decreased so that the distribution (7) of the sensitivity remains the same. That is, drivers vary their sensitivity between the same boundaries but they vary that less or more rapidly.

In order to show the changes of the distribution in a more concise way we plotted these quantities as a function of the noise strength in Fig. 5. Here each data point is a result of 5000 realizations. One can see that when varying κ, the most probable merging time $T_{\rm m}^{\rm MP}$ has a minimum around $\kappa \simeq 0.03$ while the standard deviation $\sigma_{T_{\rm m}}$ of the merging time distribution has a maximum around $\kappa \simeq 0.1$. The latter might correspond to the fact that $\kappa \simeq 0.1$ implies $\gamma \simeq 1.0$, that is, the relaxation time of the random walk is equal to the average relaxation time $1/\alpha$ and to the delay time as well.

Finally, we remark that for a small noise strength (that is, for large relaxation time) we observed collisions of vehicles for several realizations. This might be due to the fact that α_i can stray far from its mean value for long periods when the relaxation time is large (see Fig. 3(a1)). Indeed, collisions are likely to occur for $\alpha_i < 0.795$ as was shown in (Orosz *et al.*, 2005).

5. CONCLUSION AND DISCUSSION

We investigated an optimal velocity car-following model where the reaction time delay of drivers is taken into account. Stochasticity is introduced by subjecting the sensitivity of drivers to a random walk. It was shown that without the stochastic terms robust oscillations may appear that correspond to stop-and-go travelling wave solutions. These oscillations and waves are either stable (in the case of one wave) or weakly unstable (in the case of two or more waves) resulting in slow dynamics of the stop-and-go traffic jams via their front dynamics. Merging and dispersion of these waves lead to a single wave solution as $t \to \infty$.

The merging and dispersing dynamics of traffic jams is robust in the sense that it persists when stochasticiy is switched on. A 'macroscopic' random walk of fronts is obtained on the top of their nonlinear dynamics resulting in a merging/dispersion time distribution with an exponential-like tail. Furthermore, by varying the noise strength a minimal value of the most probable merging/dispersion time is found which is smaller than the merging time in the deterministic model.

Here stochasticity was introduced in such a way that drivers may still be considered identical in terms of their sensitivity distribution. An alternative (perhaps more realistic) approach might be for α_i to be sampled from different distributions so as to model different driver/vehicle classes. However, even when the $\alpha_i(t) \equiv \alpha_i$ are time dependent but different from each other the full periodic solution structure of the $\alpha_i(t) \equiv \alpha$ case may not be inherited. The resulting dynamics is an interesting challenge for future research.

REFERENCES

Engelborghs, K., T. Luzyanina and G. Samaey (2001). DDE-BIFTOOL v. 2.00: A Matlab package for bifurcation analysis of delay differential equations. Technical Report TW-330. Department of Computer Science, Katholieke Universiteit Leuven, Belgium. `http://www.cs.kuleuven.ac.be/~koen/delay/ddebiftool.shtml`.

Finch, S. R. (2004). Ornstein-Uhlenbeck process, Tutorial. `http://pauillac.inria.fr /algo/csolve/ou.pdf`.

Green, K., B. Krauskopf and K. Engelborghs (2004). One-dimensional unstable eigenfunction and manifold computations in delay differential equations. *Journal of Computational Physics* **197**(1), 86–98.

Helbing, D. (2001). Traffic and related self-driven many-particle systems. *Reviews of Modern Physics* **73**(4), 1067–1141.

Kerner, B. S. (1999). The physics of traffic. *Physics World* (August), 25–30.

Noskowicz, S. H. and I. Goldhirsch (1990). First-passage-time distribution in a random walk. *Physical Review A* **42**(4), 2047–2064.

Orosz, G. and G. Stépán (2006). Subcritical Hopf bifurcations in a car-following model with reaction-time delay. *Proceedings of the Royal Society of London A, Published Online*. `http://www.journals.royalsoc.ac.uk/openurl.asp?genre =article&id=doi:10.1098/rspa.2006.1660`.

Orosz, G., B. Krauskopf and R. E. Wilson (2005). Bifurcations and multiple traffic jams in a car-following model with reaction-time delay. *Physica D* **211**(3-4), 277–293.

Orosz, G., R. E. Wilson and B. Krauskopf (2004). Global bifurcation investigation of an optimal velocity traffic model with driver reaction time. *Physical Review E* **70**(2), 026207.